Synthesis of Oxygen-Deficient Indium−Tin-Oxide (ITO) Nanofibers

X. S. Peng,* G. W. Meng, X. F. Wang, Y. W. Wang, J. Zhang, X. Liu, and L. D. Zhang

Institute of Solid State Physics, Chinese Academy of Sciences, Hefei 230031, P. R. China

Received April 3, 2002
Revised Manuscript Received July 29, 2002

The novel properties of one-dimensional (1D) nanostructure materials have attracted extensive interest over the last decade due to their great potential for addressing some basic issues about dimensionality and size-confined transport phenomena, as well as applications in nanosensors,[1,2] logic gates, and computations.[3,4] Aside from nanotubes,[4] various nanowires (nanorods) have been fabricated by using different methods such as laser ablation,[5] templating,[6] arc discharge,[7] vapor-phase transport,[8] and solution method.[9] Recently, much attention has been paid to the preparation of nanostructures of the family of oxides for their interesting optical and electronical properties. Several oxide nanowires such as MgO,[10] SiO_2,[11] Ga_2O_3,[7] GeO_2,[12] ZnO,[13] and In_2O_3,[14] and nanobelts such as Ga_2O_3, In_2O_3, CdO, and ZnO,[15] have been successfully synthesized. However, the compositions of all these 1D oxide nanostructures are binary oxide. Here, ternary oxide fibers, Sn-doped In_2O_3 nanofibers, were synthesized.

Tin-doped In_2O_3 (ITO), a wide band gap transparent semiconductor (E_g = 3.5−4.3 eV), is an ideal material for flat-panel displays because of its high electrical conductivity and highly optical transparency,[16] and it can also be used for gas sensors.[17] The current studies mainly focus on the preparation and properties of ITO thin films.[18,19] ITO whiskers were synthesized on a glass substrate by the electron shower physic-vapor-deposition (PVD) from ITO target.[20,21] However, the aspect ratio (length to diameter) of these whiskers was small and the synthesis method was complex. In this study, we demonstrate an efficient and simple route for the synthesis of ITO nanofibers entailing a rapid heating process in argon/oxygen atmosphere from a mixture comprising indium and tin. It has been found that tin plays a crucial role in directing the growth of the ITO nanofibers based on the vapor−liquid−solid (VLS) mechanism.

The detailed experimental procedure is as follows: a mixture of indium (99.99%) 90 at. % and tin (99.99%) 10 at. % grains, was placed on a ceramic boat, and put into a ceramic tube (25 mm i.d.). The apparatus used was a horizontal electronic resistance furnace heated by silicon−carbon rods. The system was rapidly heated to 900 °C, and kept at this temperature for 60 min for product 1; heated to 1000 °C and maintained for 60 min for product 2; heated to 1100 °C and held for 60 min for product 3; and heated to 900 °C and held for 90 min for product 4. A constant flow of gas mixture (argon/oxygen, 9:1) at a flow rate of 200 sccm was maintained during the experiment process. After the system had cooled to room temperature, a large piece of transparent, wool-like product was collected from the inner wall of the ceramic tube at the downstream end. The products were characterized by x-ray diffraction (XRD) (PW 1710 instrument with Cu Kα radiation), scanning electronic microscopy (SEM) (JEOL JSM 6300), high-resolution transmission electronic microscopy (HRTEM) (JEOL 2010, operated at 200 kV), energy-dispersive X-ray fluorescence (EDX) (EDAX, DX-4) attached to the JEOL 2010, and a MKII X-ray photoelectron spectroscopy (XPS) instrument (employing Mg Kα, E = 1253.6 eV). For SEM observations, the product was pasted on the Al substrate by carbon conducting paste. Specimens for TEM and HRTEM investigation were briefly ultrasonicated in ethanol, and then a drop of suspension was placed on a holey copper grid with carbon film.

The morphologies of the products synthesized under different conditions were examined by SEM. The corresponding morphologies of products 1, 2, 3, and 4 are shown in Figure 1a, b, c, and d, respectively. It can be seen that the ITO nanofibers grew larger with the increasing deposition time; at the same time, the surface of the nanofibers varied from uniform straight (Figure 1a) to rough (Figure 1d). There also exist some smaller ITO needles on the surface of the larger ITO fibers (Figure 1d). These results were also confirmed by TEM investigation (Figure 3d). The morphologies (Figure 1a−c) also varied from circular wire (Figure 1a) to flake (Figure 1b) and rectangular column (Figure 1c) with different temperatures. These nanofibers are in diameters of several tens to several hundreds nm and in lengths of several μm to tens even hundreds of μm.

* To whom correspondence should be addressed. Fax: +86-551-5591434. E-mail: zyzhao@mail. issp. ac. cn.

(1) Cui, Y.; Wei, Q.; Park, H.; Lieber, C. M. *Science* **2001**, *293*, 1289.
(2) Favier, F.; Walter, E. C.; Zach, M. P.; Benter, T.; Penner, R. M. *Science* **2001**, *293*, 2227.
(3) Huang, Y.; Duan, X.; Cui, Y.; Lauhon, L. J.; Kim, K.-H.; Lieber, C. M. *Science* **2001**, *294*, 1313.
(4) Bachtold, A.; Hadley, P.; Nakanishi, T.; Dekker, C. *Science* **2001**, *294*, 1317.
(5) Duan, X.; Lieber, C. M. *Adv. Mater.* **2000**, *12*, 298.
(6) Li, Y.; Meng, G. W.; Zhang, l. D.; Phillipp, F. *Appl. Phys. Lett.* **2000**, *76*, 2011.
(7) Choi, Y. C.; Kim, W. S.; Park, Y. S.; Lee, S. M.; Bae, D. J.; Lee, Y. H.; Park, G. S.; Choi, W. B.; Lee, N. S.; Kim, J. M. *Adv. Mater.* **2000**, *12*, 746.
(8) Wu. Y.; Yang, P. *Chem. Mater.* **2000**, *12*, 605.
(9) Trentlet, T. J.; Hickmans, K. M.; Goel, S. C.; Viano, A. M.; Gibbons, P. C.; Buhro, W. E. *Science* **1995**, *270*, 1791.
(10) Yang, P.; Lieber, C. M. *Science* **1996**, *273*, 1836.
(11) Wang, Z. L.; Gao, R. P.; Gole, J. L.; Stout, J. D. *Adv. Mater.* **2000**, *12*, 1938.
(12) Bai, Z. G.; Yu, D. P.; Zhang, H. Z.; Ding, Y.; Gai, X. Z.; Hang, Q. L.; Xong, G. C.; Feng, S. Q. *Chem. Phys. Lett.* **1999**, *303*, 311.
(13) Hang, M. H.; Wu, Y.; Feick, H.; Tran, N.; Weber, E.; Yang, P. *Adv. Mater.* **2001**, *13*, 113.
(14) Liang, C.; Meng, G.; Lei, Y.; Phillipp, F.; Zhang, L. *Adv. Mater.* **2001**, *13*, 1330.
(15) Pan, Z. W.; Dai, Z. R.; Wang, Z. L. *Science* **2001**, *291*, 1947.
(16) Ginley, D. S.; Bright, C. *Mater. Res. Soc. Bull.* **2000**, *25*, 15.
(17) Sberveglieri, G.; Faglia, G.; Gropplli, S.; Nelli, P. *Sens. Actuators, B* **1992**, *5*, 79.
(18) Wang, Z.; Hu, X. *Thin Solid Films* **2001**, *392*, 22.
(19) Kim, H. J.; Bae, J. W.; Kim, J. S.; Kim, K. S.; Jang, Y. C.; Yeom, G. Y.; Lee, N.-E. *Thin Solid Films* **2000**, 377−378, 115.
(20) Yumoto, H.; Sako, T.; Gotoh, Y.; Nishiyama, K.; Kaneko, T. *J. Cryst. Growth* **1999**, *203*, 136.
(21) Yumoto, H.; Hatano, J.; Watanabe, T.; Fujikawa, K.; Sato, H. *Jpn. J. Appl. Phys.* **1993**, *32*, 1204.

10.1021/cm025567o CCC: $22.00
Published on Web 10/23/2002

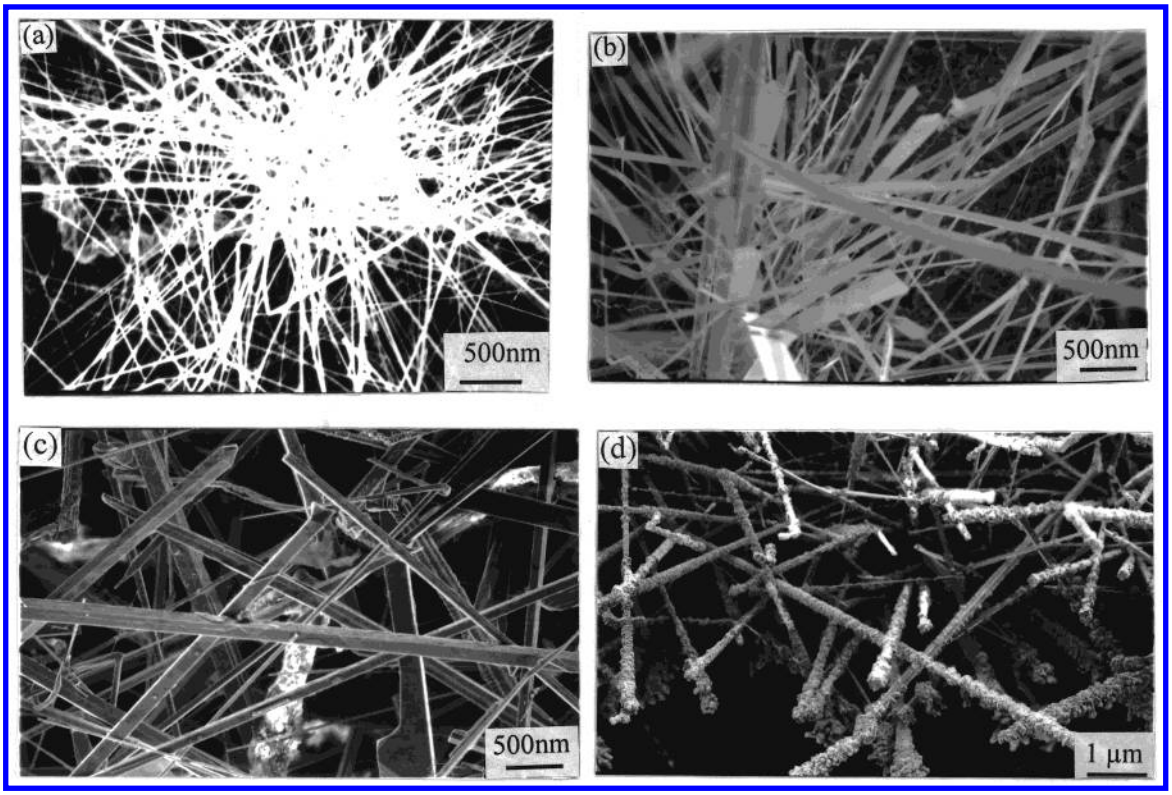

Figure 1. Typical SEM images of the ITO nanofibers prepared from different deposition conditions: (a) 60 min (900 °C); (b) 60 min (1000 °C); (c) 60 min (1100 °C); and (d) 90 min (900 °C).

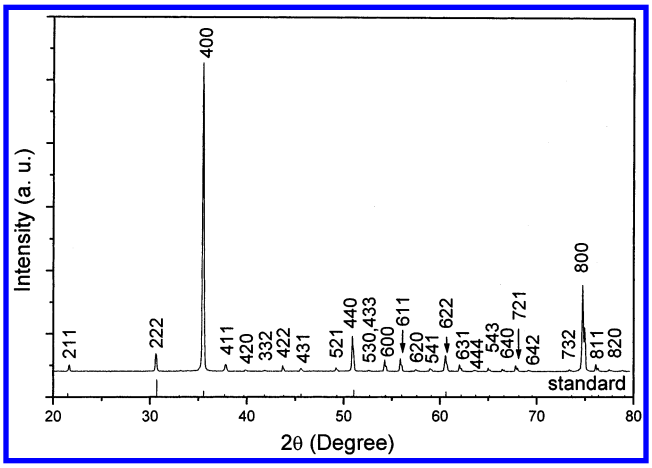

Figure 2. XRD patterns of product 1.

XRD was used to examine the crystal and phase purity of product 1 (Figure 2). We also measured the XRD patterns of the other products. All the relatively sharp diffraction peaks can be indexed to a body-centered cubic (bcc) structure with lattice constant of $a = 10.10$ nm, which is consistent with the standard value for bulk cubic-In_2O_3 (JCPDS 6-0416). In addition, comparing the intensities of the (400), (600), (800), and (222) peaks of the nanofibers with those of the standard bulk bcc-In_2O_3, we found that the relative intensities of (400), (600), and (800) peaks have been dramatically improved. These results indicate that the nanofibers may have a preferential [100] growth direction. This can be further confirmed by HRTEM and the corresponding selected area electron diffraction (SAED).

The morphology, structure, and composition of the individual ITO nanofibers have been characterized in further detail using TEM and EDX. Figure 3a shows several wire-like nanofibers and a representative image of one nanofiber capped with a nanoparticle (insert in Figure 3a) from product 1. The attached nanoparticles show up dark. EDX analysis (Figure 3b and c) indicates that the nanoparticles are composed of Sn 16.31 at. %, In 23.92 at. % and O 59.77at. %, whereas the stem of the nanofibers consists of Sn 4.63at. %, In 40.24at. %, and O 55.13 at. %, in good agreement with the corresponding ratio of ITO thin films (In/Sn, 9:1). The presence of Sn-rich In−Sn−O nanoparticles at the end of the nanofibers represents strong evidence for a growth process dominated by the VLS mechanism. A typical TEM image of product 4, Figure 3d, reveals that there are three smaller needles generated from the larger one. This result also demonstrates that when the nanofibers grow large enough some small needles will generate from their surface. Furthermore, the corresponding HRTEM image (Figure 4b) and SAED pattern recorded along the [1$\bar{3}$0] zone axis (inset in Figure 4b) of an individual nanofiber (Figure 4a) reveal that the ITO nanofiber is single-crystalline with [100] growth direction, and also with a rough surface in atomic scale. In this picture, the nanocrystal lattice fringes are spaced 0.253 nm apart. This finding is in agreement with the d value of the (400) planes of the In_2O_3 crystal. We have carried out extensive investigations on more individual nanofibers from products 1, 2, 3, and 4 with HRTEM and EDX, and the results demonstrate that the synthesized ITO nanofibers have a preferable [100] growth direction and composite of In, Sn, and O elements.

The VLS crystal growth mechanism, in which the main feature is the presence of intermediates that serve as catalysts between the vapor feed and the solid growth

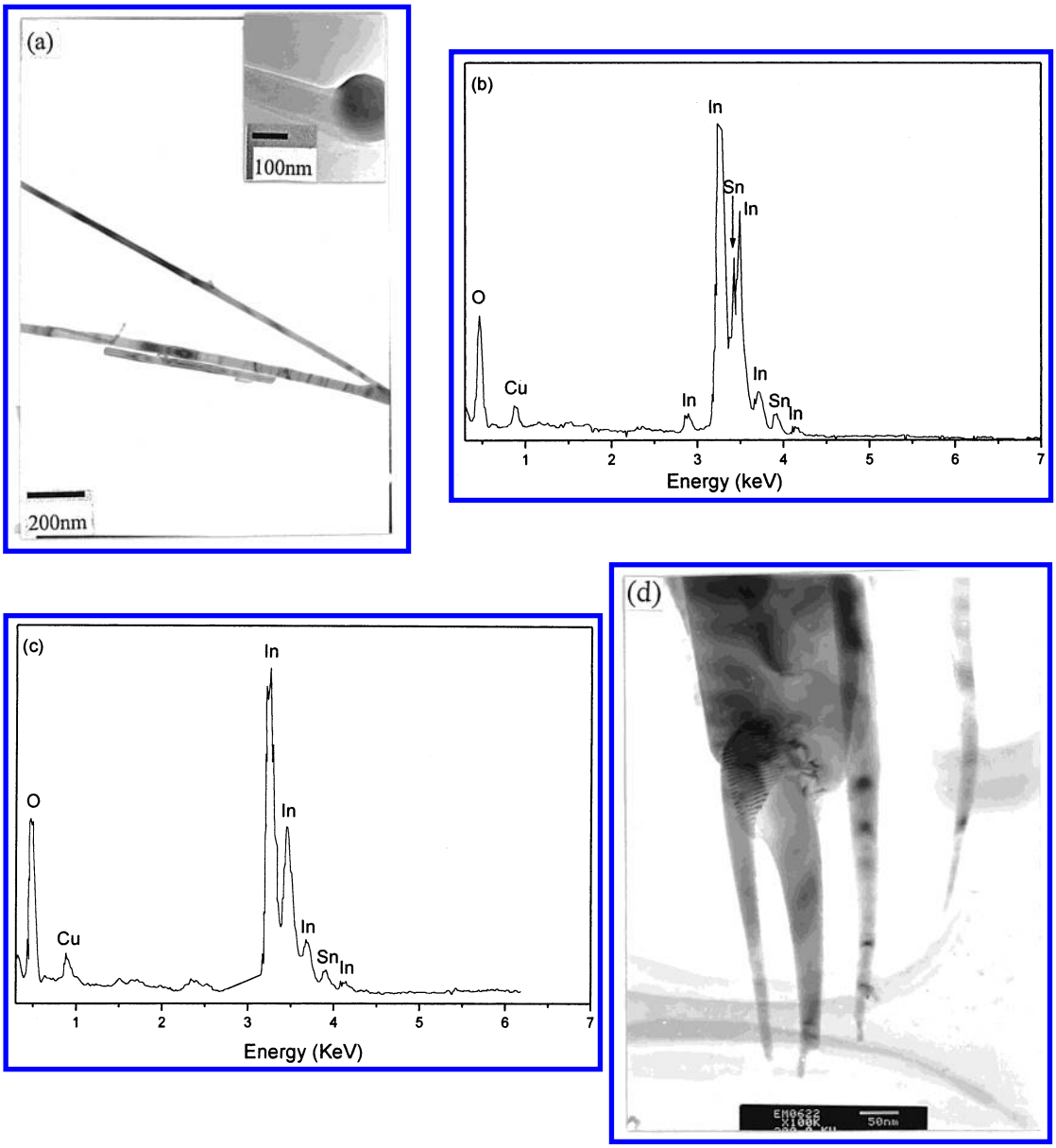

Figure 3. (a) TEM image of an individual ITO nanofiber ending with a nanoparticle from product 1; (b) and (c) are the EDX analysis results of the nanoparticle and the stem of the nanofiber, respectively. (d) Three smaller nanofibers generating from the larger one.

at elevated temperature, and the morphology feature is a catalyst particle located at the end of the nanowire, has been widely used for the growth of semiconductor nanowires such as Si,[5] GaN,[22] GaAs, and InAs.[23] Recently, oxide semiconductor nanowires such as ZnO have also been synthesized via the VLS growth mechanism.[13] In our experiment, the vapor molecules are In, Sn, and O_2. The In−Sn−O ternary phase diagram shows that both In_2O_3 and the Sn-rich liquid phase can coexist.[24] When a Sn-rich droplet is supersaturated by the vapor molecules, In_2O_3 precipitates and In_2O_3 whiskers can grow via VLS mechanism.[20,21] In the present studies, the growth of ITO nanofibers may involve the following steps. At the beginning, In−Sn liquid alloy can form at about 200 °C. As the temperature increased, more In and Sn vapors with high vapor pressure are generated from the In and Sn liquid alloys. Then, the oxidation process took place and formed In−Sn−O ternary phase. Subsequently, when a Sn-rich droplet is supersaturated by the vapor molecules, In_2O_3 precipitates, and crystalline nanofiber can grow, resulting in reducing the free energy of the liquid−solid system. At the same time, some Sn atoms diffused and doped into these In_2O_3 nanofibers. Now, the concentration of Sn in the stem of the nanofibers (Figure 3b) becomes lower than that on the tip droplet (Figure 3c). These results demonstrate that In_2O_3 nanofibers are doped by Sn, namely ITO nanofibers are formed. Simultaneously, there are also some In_2O_3 molecules detached from the surface of the nanofibers previously formed, which may be responsible for the formation of a nanofiber with rough surface as shown in the HRTEM investigation. In addition, with the deposition time

(22) Duan, X. F.; Lieber, C. M. *J. Am. Chem. Soc.* **2000**, *122*, 188.
(23) Yazawa, M.; Koguchi, M.; Muto, A.; Hiruma, K. *Adv. Mater.* **1993**, *5*, 557.
(24) Frank, G.; Brock, L.; Bausen, H. D. *J. Cryst. Growth* **1976**, *36*, 179.
(25) Fan, J. C. C.; Goodenough, J. B. *J. Appl. Phys.* **1977**, *48*, 3524.

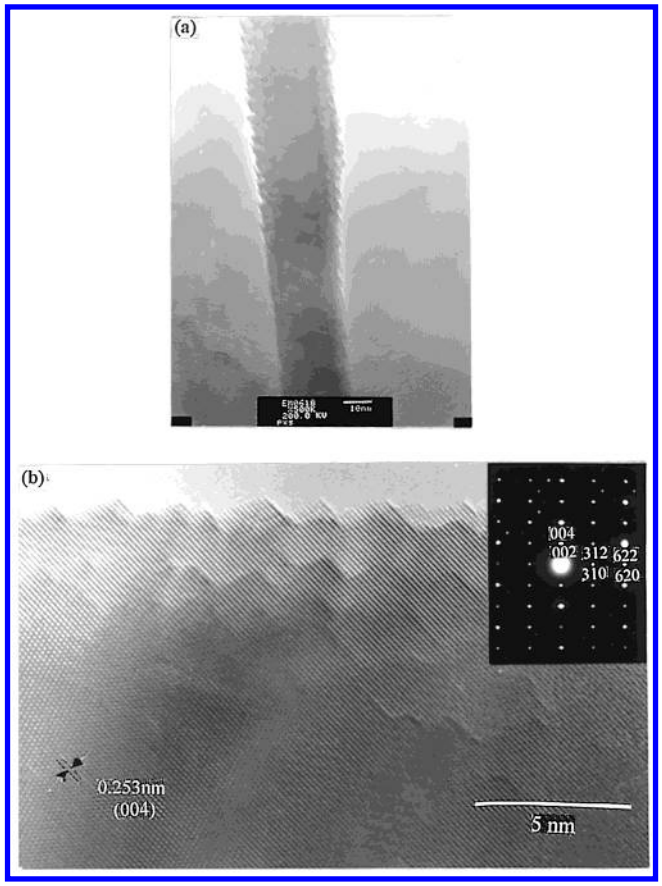

Figure 4. (a) TEM image of a single ITO nanofiber, and (b) the corresponding HRTEM image. The inset is the SAED pattern recorded along the [1$\bar{3}$0] zone axis.

increasing, some small droplets deposit on the surface of large nanofibers, directing the formation of smaller needles on the surface of larger fibers. As for the growth mechanisms for the products 2 and 3, these were unclear. One plausible explanation is that VLS takes place only at the droplet base, and this initiation core develops through vapor−solid (VS) deposition from the droplet to the fiber edges, thus forming the flakelike and rectangle fibers.

XPS was also used to determine the composition of our products. Figure 5 shows the corresponding XPS spectra of O_{1s} (Figure 5a), $In_{3d5/2}$ (Figure 5b) and $Sn_{3d5/2}$ (Figure 5c). The spectrum (Figure 5a) is disconvoluted into two peaks by the best fitting with Gassian function. Peak 1 at 529.87 eV is due to bulk O^{2-} ions whose neighboring In atoms had a full complement of six nearest O^{2-} ions, and peak 2 at 532.38 eV is corresponded to O^{2-} ions in oxygen deficiency regions.[20,24] Thus, it can be concluded that oxygen deficiencies exist in our ITO nanofibers. Furthermore, in Figure 5b, the peak energy of $In_{3d5/2}$ was lowered slightly from 444.8 eV (In_2O_3), to 444.4 eV. The binding energy of $Sn_{3d5/2}$ (Figure 5c) was 486.0 eV lower than that of tin oxide (>486.4 eV). These results further confirmed that these ITO nanofibers were oxygen deficient because the oxygen deficiency decreases the binding energy of In and Sn.[20,24]

In summary, we have synthesized ITO nanofibers by using a thermal evaporation−oxidation method. The growth involves a VLS crystal growth mechanism from the Sn-riched In−O−Sn ternary alloys droplet. Not only

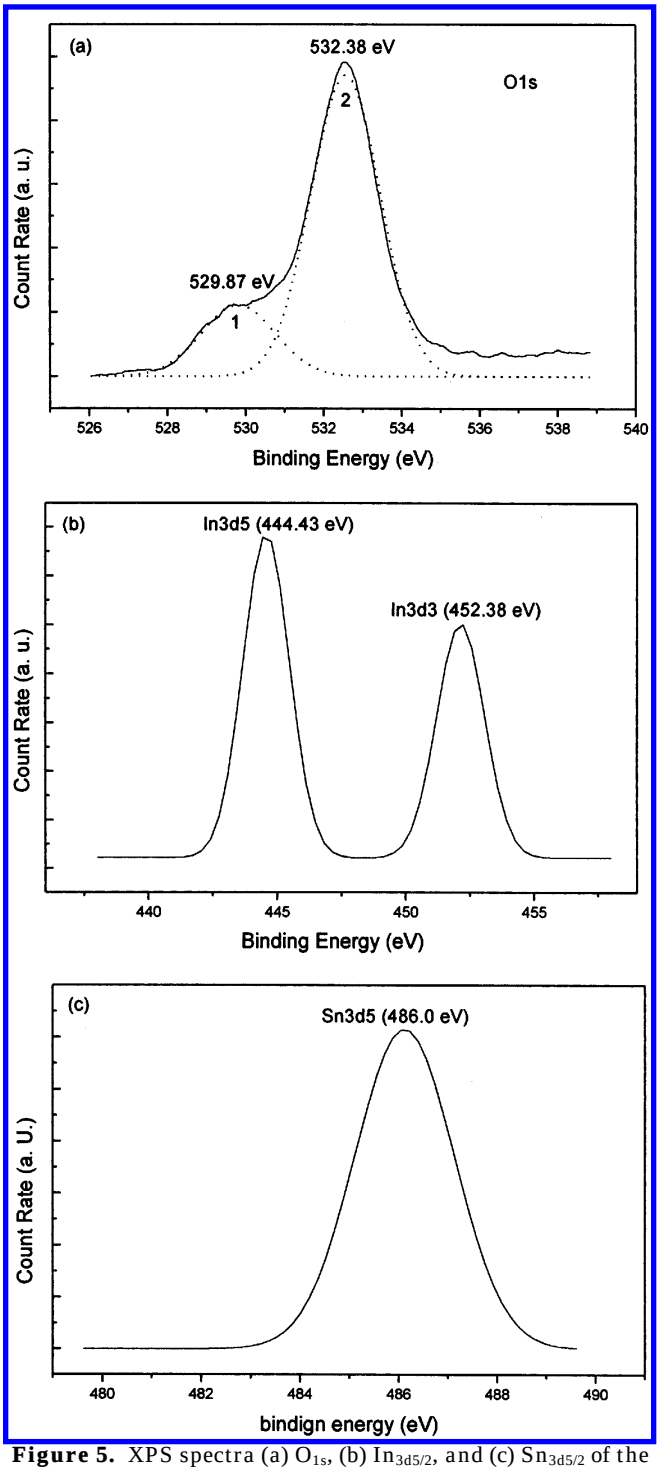

Figure 5. XPS spectra (a) O_{1s}, (b) $In_{3d5/2}$, and (c) $Sn_{3d5/2}$ of the ITO nanofibers prepared for 60 min at 900 °C.

the diameters, but also the surface morphologies, of ITO nanofibers can be controlled by the deposition conditions such as time and temperature. The XPS spectra of the ITO nanofibers show that a large amount of oxygen deficiencies exist in these nanofibers. The synthesized ITO nanostructures with different morphologies should have potential applications in optoelectronic nanodevices and nanosized gas sensors.

Acknowledgment. This work was supported by the Ministry of Science and Technology of China (Grant G1999064501) and Natural Science Foundation of China (Grant 19974055)

CM025567O